Thermal simulations in the human head for high field MRI using parallel transmission

Aurélien MASSIRE[1], Martijn CLOOS[1,2], Michel LUONG[2], Alexis AMADON[1], Alexandre VIGNAUD[3], Christopher J. WIGGINS[1], Denis LE BIHAN[1], and Nicolas BOULANT[1]

[1]DSV I2BM NeuroSpin, CEA, Gif-sur-Yvette, France, [2]DSM IRFU SACM, CEA, Gif-sur-Yvette, France, [3]Siemens Healthcare, Paris, France

Introduction: To ensure patient safety, IEC [1] states that the localized temperature in the head and that the temperature rise in the eyes should not exceed 39 °C and 1 °C respectively. Numerical simulations were performed to investigate the compliance of the specific absorption rate (SAR) versus the temperature guidelines for the human head in MRI procedures utilizing parallel transmission at 7 T, i.e. at 297 MHz. Computations using finite elements (FE) and finite difference time domain (FDTD) techniques have been implemented on an updated version of human head model [2]. Temperature evolution throughout the head was calculated by integrating numerically the Pennes' bioheat equation [3] for 1000 parallel transmission scenarios corresponding to random static RF configurations, for the synthesized circularly polarized (CP) mode, and for two realistic Transmit-SENSE RF exposures corresponding to standard MRI exam sequences : the MP-RAGE and a multi-slice T1-GRE sequence.

Materials & Methods: The head coil used in this study consisted of eight stripline dipoles distributed every 42° on a cylindrical surface with 27.6-cm diameter, leaving an open space in front of the eyes for fMRI. All dipoles were tuned and matched ideally at 297 MHz with the head model loaded in the coil. Data obtained from [1] was used to generate a new surface-based human head model made of 20 anatomical structures entities (ASE) with specific electrical and thermal properties. Resulting electrical and magnetic field maps were interpolated onto a 2.5 × 2.5 × 2.5 mm^3 resolution Cartesian grid for FDTD-based (5 sec time-step) SAR and thermal computations. The temperature distribution was obtained by integrating numerically the Pennes' bioheat equation with temperature-dependent parameters:

$$\rho.Cp\frac{\partial T}{\partial t} = \vec{\nabla}(k\,\vec{\nabla}T) + \rho.SAR + Q - B[T - Tb],$$

where ρ is the ASE density in kg/m^3, C_p the specific heat in J/kg/K, T the local temperature in Kelvin, k the thermal conductivity in W/m/K, Q the metabolic rate in W/m^3 and B the perfusion coefficient in $W/m^3/K$. The boundary conditions included convection, sweat and radiation. The blood temperature is Tb, here considered to be constant in time and equal to the core temperature (i.e. 37 °C). The ambient temperature of the air surrounding the subject was set to 24 °C. An equilibrium temperature distribution was first calculated with no SAR source. To have a representative sample of the possible SAR and heating patterns one may obtain in parallel transmission, 1000 static RF configurations were simulated by generating random phases for each coil channel while keeping their amplitude equal, the CP-mode being a particular case. The SAR maps, with their corresponding global and peak 10-g averages were calculated. The statistics of their ratio (SAR_L/SAR_W) was also computed as it is sometimes used in worst-case scenarios or to see possible trends between global-local SAR relationships. The temperature was calculated for ½ hour of RF exposure scaled corresponding either to the global SAR or the 10-g average local SAR limits (separate simulations) specified in the latest IEC guidelines, i.e. 3.2 and 10 W/kg respectively. Temperature evolution throughout the head was also simulated for standard MRI sequences: a magnetization-prepared rapid gradient echo (MP-RAGE) and an axial multi-slice T1 gradient recalled echo (T1-GRE) sequence lasting 12 minutes each, where all pulses had been designed to yield normalized root mean square errors on the flip angle less than 5% over the entire brain regions using the spokes [4] and the k_T-points [5] methods.

Results & Discussion: The mean, standard deviation, minimum and maximum values of the SAR_L/SAR_W ratios histogram for the 1000 scenarios simulated were 9.2, 2.4, 4.2 and 19.5 respectively. Because of its proximity to the coil elements, the maximum local SAR was found in the skin in 66 % of the cases, the remaining 34 % being found in the CSF due to its high conductivity. The 10-g average SAR limit was always reached first. In such a case, the local temperature did not exceed 37.7 °C in more than 90 % of the 1000 scenarios (see Figure 1), even after 30 minutes of RF exposure. The maximum temperature rise in the eyes was larger than 1 °C in 20 % of the cases, the shortest duration to reach this value being 7 minutes. When the SAR maps were scaled up to reach 3.2 W/kg for the head average, over half of the 1000 scenarios exceeded 38 °C in just 6 minutes of RF exposure, the maximal temperature usually rising up to 39 °C for 40 % of the cases after 30 minutes. The simulations of the CP-mode yielded a lower SAR_L/SAR_W ratio so that both local and global SAR limits were reached simultaneously. All temperature guidelines in this case were respected. Two examples of 10-g SAR and temperature rise maps are provided in Figure 2. Whereas the local 10-g limit of 10 W/kg throughout this study seemed to be a good guide to ensure that a temperature of 38 °C would almost never be reached, it certainly seems quite conservative when considering the new temperature guideline of 39 °C [1]. If this temperature is now deemed a safe limit for the "normal" mode, the simulations reported here then show that the SAR constraints could probably be relaxed. On the other hand, we found that even with 10 W/kg as the maximum 10-g average SAR, the maximum temperature rise in the eyes could be above 1 °C. Thermal simulations performed for the realistic MRI sequences also confirm that the SAR limits seem conservative compared to the temperature ones, with the maximum temperatures reached being 37.6 and 37.5°C for the MP-RAGE and T1-GRE respectively.

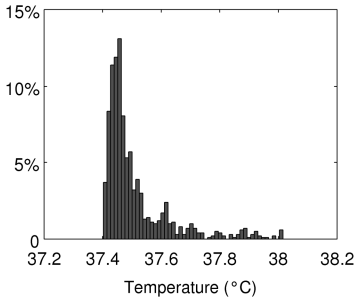

Figure 1: Maximum local temperature histogram (30 minutes of RF exposure, SAR_L = 10 W/kg) for the 1000 static RF phase configurations.

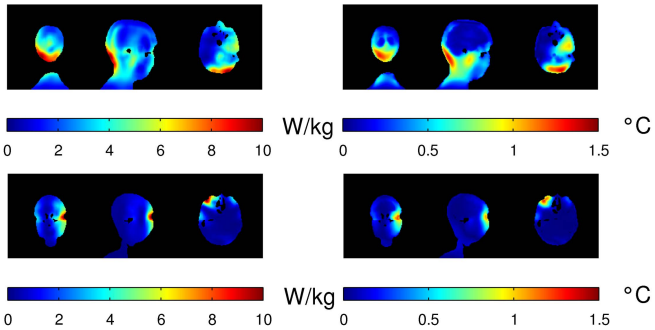

Figure 2: Top row: Local 10-g average SAR distribution and corresponding local rise in temperature after a 30 minute RF exposure when SAR_L = 10 W/kg for a low (4.42) SAR_L/SAR_W ratio static RF configuration. **Bottom row:** Local 10-g average SAR distribution and corresponding local rise in temperature after a 30 minute RF exposure when SAR_L = 10 W/kg for a high (19.47) SAR_L/SAR_W ratio static RF configuration. From left to right in each figure are shown coronal, sagittal and axial slices going through the 10-g SAR hot spot.

Conclusion: Based on Pennes' bioheat equation, using recommended values of 10 W/kg for local 10-g average SAR in parallel transmission, our simulations seem to indicate that, with our setup, the local temperature inside the human head never exceeds 39 °C (and barely 38 °C), but temperature rises larger than 1 °C may occur in the eyes.

References: [1] International Electrotechnical Commission 2010:601:2-33. [2] N. Makris et al. Med Biol Eng Comput 2008:46:1239-1251. [3] HH. Pennes. J Appl Physiol 1948:1:93-122. [4] S. Saekho et al. Magn Reson Med 2006:55:719–724. [5] MA. Cloos et al. Magn Reson Med 2011:DOI:10.1002/mrm.22978.